Internal defect and process parameter analysis during friction stir welding of Al 6061 sheets

4 authors:

Perumalla JANAKI Ramulu
Adama Science and Technology University
68 PUBLICATIONS **286** CITATIONS

SEE PROFILE

Ganesh Narayanan
Indian Institute of Technology Guwahati
99 PUBLICATIONS **758** CITATIONS

SEE PROFILE

Satish Vasu Kailas
Indian Institute of Science
263 PUBLICATIONS **4,812** CITATIONS

SEE PROFILE

Jayachandra Reddy
Tenneco
4 PUBLICATIONS **92** CITATIONS

SEE PROFILE

Some of the authors of this publication are also working on these related projects:

Project   Expert Systems for predicting formability of TWBs View project

Project   Time Efficient Simulations of Plunge and Dwell Phase of FSW and its Significance in FSSW View project

ORIGINAL ARTICLE

Internal defect and process parameter analysis during friction stir welding of Al 6061 sheets

P. Janaki Ramulu · R. Ganesh Narayanan ·
Satish V. Kailas · Jayachandra Reddy

Abstract Welding parameters like welding speed, rotation speed, plunge depth, shoulder diameter etc., influence the weld zone properties, microstructure of friction stir welds, and forming behavior of welded sheets in a synergistic fashion. The main aims of the present work are to (1) analyze the effect of welding speed, rotation speed, plunge depth, and shoulder diameter on the formation of internal defects during friction stir welding (FSW), (2) study the effect on axial force and torque during welding, (c) optimize the welding parameters for producing internal defect-free welds, and (d) propose and validate a simple criterion to identify defect-free weld formation. The base material used for FSW throughout the work is Al 6061T6 having a thickness value of 2.1 mm. Only butt welding of sheets is aimed in the present work. It is observed from the present analysis that higher welding speed, higher rotation speed, and higher plunge depth are preferred for producing a weld without internal defects. All the shoulder diameters used for FSW in the present work produced defect-free welds. The axial force and torque are not constant and a large variation is seen with respect to FSW parameters that produced defective welds. In the case of defect-free weld formation, the axial force and torque are relatively constant. A simple criterion, $(\partial \tau / \partial p)_{\text{defective}} > (\partial \tau / \partial p)_{\text{defect free}}$ and $(\partial F / \partial p)_{\text{defective}} > (\partial F / \partial p)_{\text{defect free}}$, is proposed with this observation for identifying the onset of defect-free weld formation. Here F is axial force, τ is torque, and p is welding speed or tool rotation speed or plunge depth. The same criterion is validated with respect to Al 5xxx base material. Even in this case, the axial force and torque remained constant while producing defect-free welds.

Keywords Friction stir welding · Defects · Welding speed · Rotational speed · Plunge depth · Shoulder diameter

Nomenclature

FSW	Friction stir welding
FSP	Friction stir processed
SD	Shoulder diameter
PD	Plunge depth
TRS	Tool rotational speed
WS	Welding speed
YS	Yield strength
UTS	Ultimate tensile strength
UE	Uniform elongation
TE	Total elongation
K	Strength coefficient
n	Strain hardening exponent
R	Plastic strain ratio
F	Axial force
τ	Torque
p	Welding speed or tool rotation speed or plunge depth

P. J. Ramulu · R. G. Narayanan (✉)
Department of Mechanical Engineering,
Indian Institute of Technology Guwahati,
Guwahati, Assam 781039, India
e-mail: ganu@iitg.ernet.in

R. G. Narayanan
e-mail: ganesh.narayanan@sify.com

S. V. Kailas · J. Reddy
Department of Mechanical Engineering,
Indian Institute of Science Bangalore,
Bangalore 560012, India

S. V. Kailas
e-mail: satvk@mecheng.iisc.ernet.in

1 Introduction

6xxx aluminum alloys are heat-treatable alloys, specifically solution heat-treated and artificially aged, and are applicable in high-strength structural members, vehicles, rolling stock,

Table 1 Chemical composition of base material (AA 6061-T651) in wt. %

Si	Fe	Cu	Mn	Mg	Cr	Zn	Ti	Al
0.65	0.3	0.27	0.02	1.0	0.17	0.04	0.02	Remaining

marine applications, architectural applications, etc. [1]. For these aluminum alloys, friction stir welding (FSW) process is a proven method for joining. In general, the process is carried out by plunging a rotating FSW tool into the inter-face of two rigidly clamped sheets until the shoulder touches the surface of the material being welded and traverse along the weld line. Welding is done with the frictional heat produced between the FSW tool and workpiece, which is the primary source of heat. The secondary heat source is the plastic deformation heat of the deforming workpiece. The frictional heat and deformation heat are utilized for bonding under the applied axial force [2, 3]. FSW process is a complex process; it has many process parameters on which the weld quality depends on. The main parameters are tool material and its geometry, welding speed, tool rotation speed, axial force, and work piece materials. The tool shape determines the heating, plastic flow, and forging pattern of the plastic weld metal and hence the weld morphology [2]. The tool material determines the rate of friction heating, tool strength, and working temperature and hence decides which materials can be friction stir-welded. Tool rotation speed is one of the main factors affecting frictional heat. If the rotating speed is too low, the frictional heat is not enough to induce plasticized flow, which leads to defects in the weld. Along with an increase of the rotating speed, frictional heat increases. The plasticized layer increases from the top to the underside, resulting in smaller defects in the weld region. When the rotating speed reaches a certain limit, the possibilities of defect formation decrease. Another main factor is welding speed. When the welding speed is too small, the frictional heat makes the temperature in the weld too high. The weld surface will be irregular. When the weld speed increases further, the material just below the tool softens to such a degree that it acts as a lubricant, lowering the friction and thus the heat input. This will reduce the temperature. Thus, in FSW, the bulk temperature does not increase beyond a certain point. But the high temperatures near the surface would result in poor surface finish due to incipient melting of this layer. The temperature in the weld

region will also be controlled by the welding speed. When the welding speed is low, the temperature rise would be higher as the heat input to a given control volume of material would be for a longer time. On the other hand, when the welding speed is too large, the frictional heat is not enough to plasticize the materials beneath the tool shoulder and around the probe, resulting in improper welding. The axial force of tool on work pieces affects the contact state and hence affects the forming of weld. When the axial force is not enough, the surface metal of the weld "floats" upward and overflows the surface of work pieces, resulting in voids at the bottom of the welding. When the axial force is too large, the frictional force increases between the tool shoulder and the workpiece surface, the tool shoulder will adhere with the base material, and there will be flash and burr on the weld face [4, 5]. This discussion shows the essentiality of proper process parameters selection before FSW for any type of base material.

The effect of tool shoulder diameter and pin profile on the mechanical properties and microstructure of 6*xxx* series alloy FSW joints has been reported in the available literature and their essentiality to fabricate good welded joints was explained. Scialpi et al. [6] studied the effect of different shoulders with scroll and fillet, cavity and fillet, and only fillet on the mechanical and microstructural properties of friction stir-welded joints of 6082 T6 aluminum alloy sheet with a thickness value of 1.5 mm. The results showed that, for thin sheets, the best joint has been welded by a shoulder with fillet and cavity. Elangovan and Balasubramanian [7] investigated the effect of tool pin profile and tool shoulder diameter on FSP zone formation in AA6061 aluminum alloy. For fabricating the FS joints, five different tool pin profiles (straight cylindrical, tapered cylindrical, threaded cylindrical, triangular, and square) with three different shoulder diameters (15, 18, and 21 mm) were used. The formation of friction stir-processed (FSP) zone has been analyzed macroscopically. Tensile properties of the joints have been evaluated and correlated with the FSP zone formation. It was found that the square pin-profile tool with 18 mm shoulder diameter produced mechanically sound and metallurgically defect-free welds compared to other tool pin profiles. Kumar and Kailas [8] investigated to understand the mechanism of friction stir weld formation and the role of friction stir welding tool in it. The results showed that there were two different modes of material flow regions involved in the friction stir weld formation, namely: "pin-driven
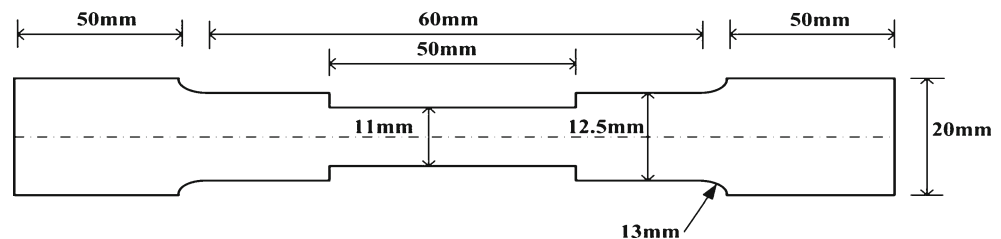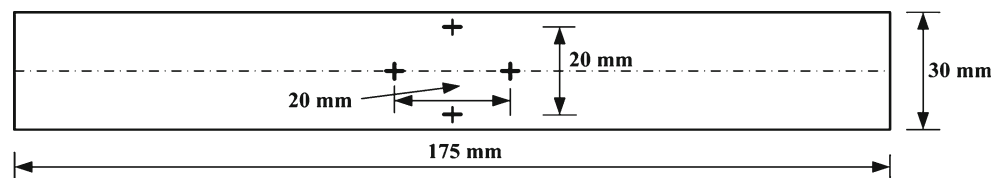

Fig. 1 Tensile test specimen dimensions as per ASTM-B557M

Fig. 2 Sheared rectangular tension test specimen, parallel strip as per ASTM-E517

flow" and "shoulder-driven flow". Both depend on the tool geometry to form defect-free joints. Similar observations are also seen in some other works [9–14], which indicates the essentiality of tool geometry during FSW for fabricating defect-free joints. In the same way, the effects of welding parameters like tool speed and welding speed on the mechanical properties and microstructure of 6xxx series alloy FSW joints are also reported [15–23]. For instance, Ren et al. [15] studied the hardness distribution, tensile properties, and fracture characteristics of 6061Al-T651 plates of 6 mm thickness. FSW was carried out at different rotation speeds (400, 600, 800, 1,200, and 1,600 rpm) and traverse speeds (100 and 400 mm/min). It was found that a higher tensile strength has been witnessed at 400 mm/min. Rodrigues et al. [16] analyzed the friction stir welds produced in 1-mm-thick plates of AA 6016-T4 aluminum alloy with two different shapes (conical and scrolled) and shoulder diameters (10 and 14 mm). The welding parameters like rotational speeds 1,800 and 1,120 rpm and welding speeds 180 and 320 mm/ min were used and compared to investigate on the evolution of microstructure and mechanical properties. It was observed from their results that the differences in tool geometry and welding parameters induced significant changes in the material flow path during welding and microstructure in the weld nugget. The tool with a conical-shaped shoulder at a rotational speed of 1,800 rpm and welding speed of 130 mm/ min has better properties. From the research work referred on FSW of 6xxx series aluminum alloys, the process parameters used for welding can be summarized as: tool shoulder diameter—10 to 24 mm, pin diameter—4 to 7.9 mm, pin length— 1.2 to 6.23 mm, tool rotation speed—300 to 3,000 rpm, and welding speed—40 to 1,100 mm/min.

It is understood from the discussion that, in general, the effect of welding parameters on the microstructure and mechanical properties are studied predominantly. A few published works have aimed at relating mainly the welding speed and rotation speed on the force and torque requirement during FSW, but not shoulder diameter and plunge depth. There is no attempt made in relating the defect formation with FSW parameters and evolution of axial force and torque during FSW. Moreover, an attempt has been made in the present work to define a simple criterion to identify the onset of defect-free region during FSW.

The main aims of the present work are to (1) analyze the effect of rotational speed, welding speed, plunge depth, and shoulder diameter on the formation of internal defects, (2) study the effect of the aforesaid parameters on the axial force and torque developed during welding, (3) optimize the welding parameters for forming defect-free welds, and (4) propose and validate a simple criterion to identify defect-free weld formation. In the present work, only butt welding of sheets was performed.

2 Experimental methodology

The base material in the present investigation is AA 6061-T651 alloy with 2.1 mm thickness. The chemical composition of the base material is given in Table 1.

The base metal was laser cut in different rolling directions like 0 °, 15 °, 30 °, 45 °, 60 °, 75 °, and 90 °, and the mechanical properties and plastic strain ratio (R) were evaluated through tensile tests as per ASTM-B557M and ASTM-E517 standards. The schematic of samples used for evaluating mechanical properties and plastic strain ratio is shown in Figs. 1 and 2, respectively. Table 2 summarizes the mechanical properties of AA 6061 base material obtained in the present work.

Table 2 Tensile properties of base metal (AA 6061-T651)

Mechanical properties	Rolling direction						
	0 °	15 °	30 °	45 °	60 °	75 °	90 °
YS (MPa)	265±5	272±7	265±4	264±15	266±12	279±8	257±17
UTS (MPa)	300±8	309±6	300±4	297±14	300±9	333±7	292±9
UE (%)	8.9	8.6	9.1	8.8	8.5	8.9	9.6
TE (%)	11.2	11.5	11.5	11.6	11.3	11.5	11.9
K (MPa)	427±30	421±15	410±7	406±17	411±10	424±10	426±15
n	0.101	0.094	0.095	0.094	0.095	0.096	0.12
R	0.79	0.74	0.78	0.95	0.84	0.93	0.85

YS yield strength, *UTS* ultimate tensile strength, *UE* uniform elongation, *TE* total elongation, *K* strength coefficient, *n* strain hardening coefficient, *R* plastic strain ratio

Fig. 3 Schematic representation of tools used for FSW
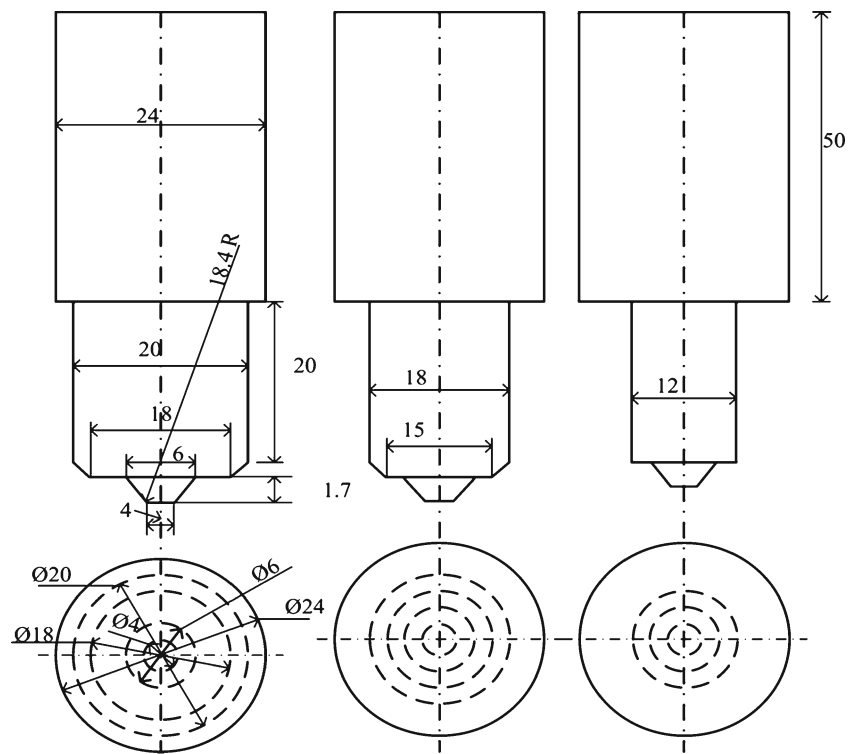
All the dimensions are in mm

Friction stir welding was carried out on a machine designed and developed by the Indian Institute of Science, Bangalore, and ETA Technologies, Bangalore. The machine had a unique capability in that the plunge depth, rotational speed, or weld speed could be varied within a test. In the present work, only one parameter was changed by keeping the other parameters constant in each experiment. The process parameters varied were tool rotational speed, welding speed, plunge depth, and shoulder diameter, while the tool tilt angle (2.5 °) was kept constant throughout the process. Three types of tools with flat shoulder having different diameters and pin with equal probe lengths were used for all the welding trials. These three tools were made of hot die steel with shoulder diameter of 12, 15, and 18 mm, pin of frustum shape with base diameter of 6 mm, top diameter of 4 mm, and length of 1.7 mm as shown schematically in Fig. 3. The base material sheets were clamped rigidly over the vertical bed from four sides to avoid vibration or displacement during processing. The welding trials were done under varied plunge depths, welding speeds, and tool rotation speeds within a specified range by three tools having different shoulder diameters as listed in Table 3. The parameter range was fixed based on the available ranges in the literature and from earlier experience such that it gives both the defect-free and defective welds. In a single trial, either plunge depth or

Table 3 Process parameters for fabricating FSW joints before optimization

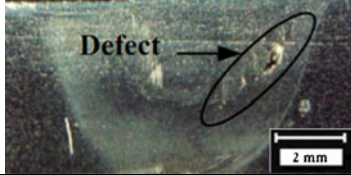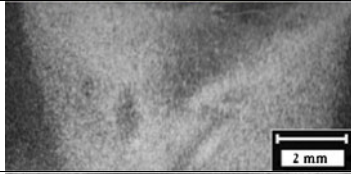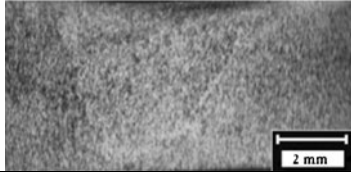| Trial	Parameters						
	Pin length (mm)	Shoulder diameter (mm)	Plunge depth (mm)		Tool rotational speed (rpm)		Welding speed (mm/min)	
			Min	Max	Min	Max	Min	Max
I	1.7	18	1.5	1.9	1,100		90	
			1.9		800	1,600		
					1,350		50	100
II		15	1.7	2.0	1,100		90	
			1.9		1,200	1,500		
					1,350		90	130
III		12	1.75	2.0	1,300		90	
			2		1,300	1,600	120	
			1.9		1,300		90	130
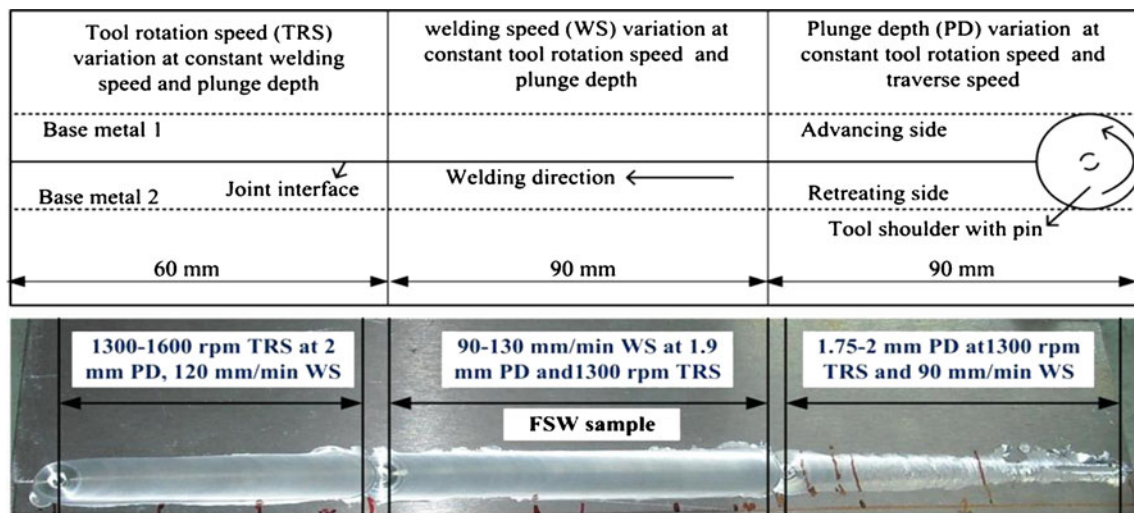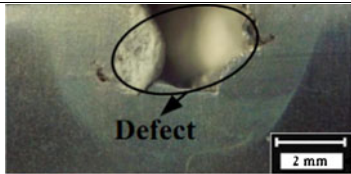
Fig. 4 *Top*, representation of process parameters variation during FSW in a single trial; *bottom*, FSW sample with varying welding parameters for 12 mm shoulder diameter

welding speed or tool rotation speed was changed for the same shoulder diameter which is shown in Fig. 4. The same has been followed for other two parameter variations also.

For example, in trial I, FSW tool with 18 mm shoulder diameter was used as listed in Table 3. All the parameters were selected such that both defective and defect-free welds are generated and with prior experience. Parameters were varied

Table 4 Macrostructures of weld region at different plunge depths

PD (mm)	Parameters	macrostructures of FSW joint	Observation
1.6	TRS:1100 rpm; WS: 90 mm/min; SD: 18 mm		Defect due to less tool plunge, insufficient heat generation and plastic deformation
1.8	TRS:1100 rpm; WS:90mm/min; SD: 18 mm		Defect due to insufficient tool plunge, heat generation and plastic deformation; Defect size is reduced
1.9	TRS: 1100 rpm; WS:90 mm/min; SD:18 mm		Defect due to insufficient tool plunge, heat generation and plastic deformation; Defect size is minimum
1.85	TRS:1300 rpm; WS:90 mm/min; SD: 15 mm		No defect
1.9	TRS:1300 rpm; WS:90 mm/min; SD: 12 mm		No defect

PD plunge depth, *TRS* tool rotation speed, *WS* welding speed, *SD* shoulder diameter

linearly during welding; due to this linearity, some of the parameters were selected in specified distances and a transverse section has been taken for internal defect characterization. The specimens for metallographic examination were sectioned to the required sizes from the joint comprising of FSW zone and base metal regions and polished using different grades of emery sheets (200–1,200 grades). Final polishing has been done using the diamond compound (1 μm in particle size) in the disc polishing machine. Specimens were etched with 1:20 of hydro fluoric (HF) acid and distilled water mixture. Specimens were examined in a stereomicroscope and all the macrostructures were captured at different process parameters. From these macrostructures, FSW joints were observed for presence of defects. During each trial, the axial force and torque were also monitored directly from the machine.

3 Results and discussion

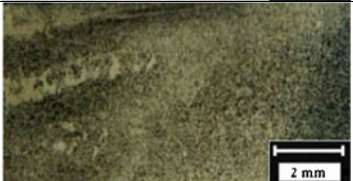### 3.1 Effect of FSW process parameters on the formation FS welds
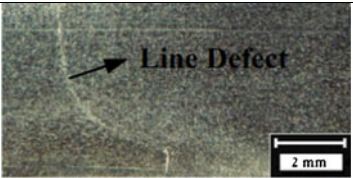
The effect of tool dimensions (like shoulder diameter) and welding parameters (welding speed, tool rotation speed, and plunge depth) on the joint quality is observed through defect analysis with an aim of fabricating defect-free joints. In general, friction stir-welded joints are known to be free from defects like porosity, slag inclusion, solidification cracks, etc., that are generated in fusion welding of aluminum alloys and these defects disintegrate the weld quality and joint properties [9]. Since FSW is a solid-state process, the base metals are joined in solid state due to the heat generated by the friction and flow of metal by the stirring action. But FSW joints are prone to other defects like pin hole, tunnel defect, piping defect, kissing bond, cracks, etc., due to improper plastic flow and insufficient consolidation of metal in the FS process region [23]. The internal defects in FS joints are observed through macrostructures at different parameter combinations. The macrostructure of the joints and parameters used are presented in Tables 4, 5, and 6.

Formation of defects at different plunge depths is shown in the Table 4. When the macrostructures are compared, defect size is more at 1.6-mm plunge depth and less at 1.9-mm plunge depth with a tool of 15 mm shoulder diameter, tool rotation speed of 1,100 rpm, and welding speed of 90 mm/min. So, with an increase in plunge depth, the defect size decreases, but the defect is not vanished. But by increasing the rotation speed to 1,300 rpm, defects are not formed even though the plunge depth and shoulder diameter are reduced.
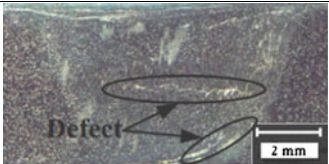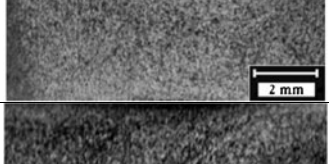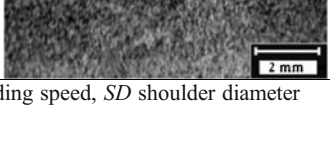
A similar exercise has been carried out for different welding speeds (Table 5) and rotation speeds (Table 6) in

Table 5 Macrostructures of weld region at different welding speeds

WS (mm/min)	Parameters	Macrostructures of FSW joint	Observation
60	TRS:1350 rpm; PD:1.9 mm; SD:18 mm		Line defect formed at the transition zone
80	TRS:1350 rpm; PD:1.9 mm; SD:18 mm		No defect
100	TRS:1350 rpm; PD:1.9 mm; SD:18 mm		No defect
120	TRS:1350 rpm; PD:1.9 mm; SD:18 mm		No defect

PD plunge depth, *TRS* tool rotation speed, *WS* welding speed, *SD* shoulder diameter

Table 6 Macrostructures of weld region at different tool rotation speeds

TRS (rpm)	Parameters	Weld zone macrostructures	Observation
900	WS:90 mm/min; PD: 1.9 mm; SD: 18 mm;		Cracks are found in the stirring zone duo incomplete plastic flow of material because of inadequate heat input at lower speeds.
1200	WS:90 mm/min; PD:1.9 mm; SD:18 mm		Small hole in stirred zone due inadequate heat input
1300	WS:90 mm/min; PD: 1.9 mm; SD: 18 mm		No defect
1400	WS:90 mm/min; PD: 1.9 mm; SD: 18 mm		No defect
1300	WS:90 mm/min; PD: 1.9 mm SD: 15 mm		No defect
1500	WS:90 mm/min; PD: 1.9 mm; SD: 15 mm		No defect

PD plunge depth, *TRS* tool rotation speed, *WS* welding speed, *SD* shoulder diameter

combination with three other parameters for generating defect-free FS welds. In a nutshell, by varying different FSW parameters, the force and torque required for generating defect-free FS welds are attained and hence proper stirring action and material plastic deformation occur during welding. The formation of defects is mainly because of improper combination of welding parameters, resulting in insufficient stirring action and plastic deformation.

Fig. 5 Variations in force and torque at variable tool rotation speed (700–1,500 rpm) by using FSW tool of 18 mm shoulder diameter, 1.9 mm plunge depth, and 90 mm/min welding speed. Error variation in force and torque is ±1 kN and ±0.5 Nm
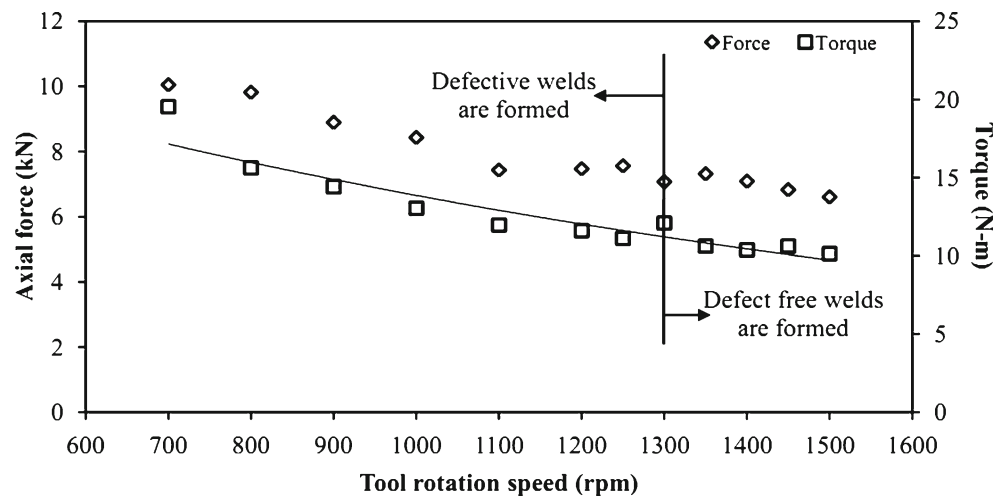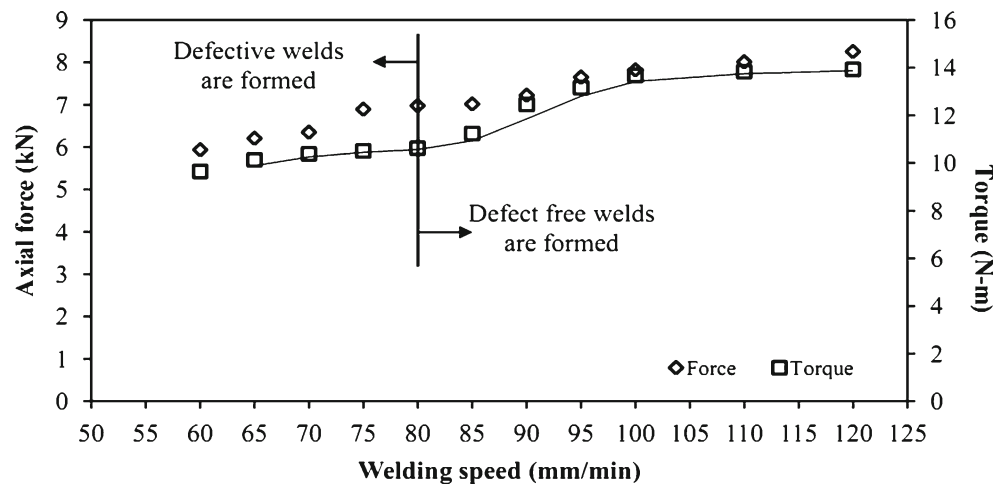
Fig. 6 Variations in force and torque at variable welding speed (60–120 mm/min) by using FSW tool of 18 mm shoulder diameter, 1.9 mm plunge depth, and 1,350 rpm tool rotation speed. Error variation in force and torque is ±1 kN and ±0.5 Nm

3.2 Effect of FSW parameters on axial force and torque during welding

The defective weld and defect-free weld formation can also be observed through the axial forces (forces in Z-direction) and their corresponding torque with respect to the four FSW parameters. The axial force is monitored through a load sensor and torque by the current and voltage from the servo motor. Figures 5, 6, 7, and 8 show the influence of varied FSW parameters on the variation of axial force and torque. The formation of the defective welds can also be related to this. It has been found from Fig. 5 that, with an increase in tool rotation speed, the axial force and torque decrease. The data given in this figure are for constant welding speed (90 mm/min), shoulder diameter (18 mm), and plunge depth (1.9 mm). It was observed in the present work, for the base material chosen, that the defective welds are formed below a tool rotation speed of 1,300 rpm, above which defect-free welds are formed. The axial force and torque requirement is substantial during welding and hence defect-free welds are formed beyond a critical limit. The decrease in axial force and torque with an increase in rotational speed is because of the heat input during welding. With an increase in heat input, the contact area below the shoulder

area or stir zone becomes softer, resulting in reduced strength in this region. The axial force and torque requirements will not be large if the strength of the stir zone is less. For good-quality welds without internal defects, higher tool rotation speed yielding lesser axial force and torque is recommended.

In the same way, the effect of variation in welding speeds (60 to 120 mm/min) using a FSW tool of 18 mm shoulder diameter and 1.9 mm plunge depth at 1,350 rpm rotation speed on the weld formation is evaluated through axial force and torque as shown in Fig. 6. The defective welds are observed up to a welding speed of 80 mm/min. It was observed that an opposite effect is seen while increasing the welding speed as compared to tool rotation speeds. By increasing the welding speed, the axial force and torque are increased. Until a critical welding speed (80 mm/min) is reached, the axial force and torque requirements are insufficient to form a defect-free weld. Once sufficient axial force and torque are reached, defect-free welds are generated. This suggests that, for defect-free welds, higher welding speeds generating higher axial forces and torques are recommended. With an increase in welding speed, heat input decreases, resulting in higher strength at stir zone. For a stronger stir zone, the axial force and torque requirements are large, leading to an increase in the magnitudes.

Fig. 7 Variations in force and torque at variable plunge depth (1.6–1.9 mm) by using FSW tool of 18 mm shoulder diameter, 1,100 rpm tool rotation speed, and 90 mm/min welding speed; defective welds are formed. Error variation in force and torque is ±1 kN and ±1 Nm
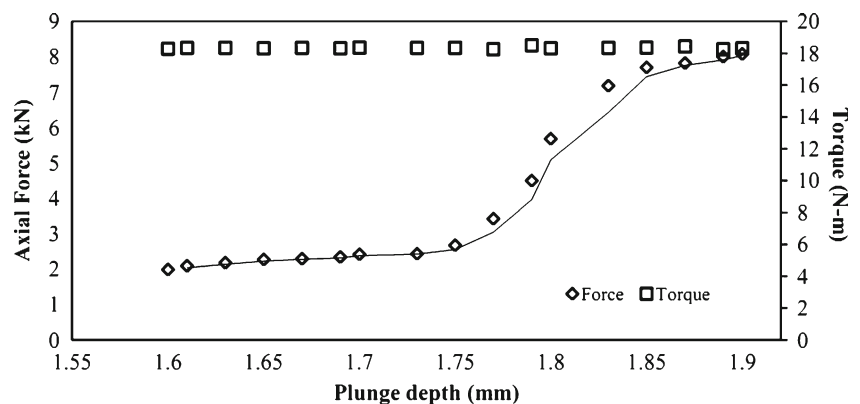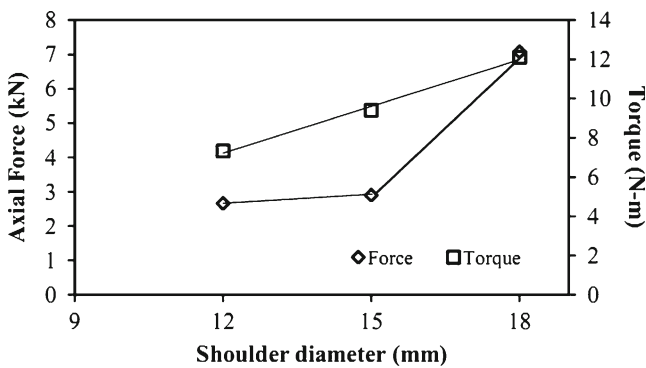
Fig. 8 Variations in force and torque at variable plunge depth (1.85–1.95 mm) by using FSW tool of 18 mm shoulder diameter, 1,300 rpm tool rotation speed, and 90 mm/min welding speed; defect-free welds are formed. Error variation in force and torque is ±1 kN and ±1 Nm

In addition to this, in the present work, the effect of pin plunge depth and shoulder diameter on axial force, torque, and defect formation is also analyzed. The axial forces and torque variations are plotted in Fig. 7 for variable pin plunge depths from 1.6 to1.9 mm by using a tool of 18 mm in shoulder diameter, 1,100 rpm tool rotation speed, and 90 mm/min welding speed. It was observed that axial force at a plunge depth of 1.6 mm is lesser, whereas at 1.9 mm plunge depth it is higher. It means that, with an increase in plunge depth, the axial force increases. But torque has not shown much variation with pin plunge depth. It remains constant for all plunge depths considered, and welds obtained with these parameter combinations are defective. With an increase in plunge depth, the reaction force given by the material to the tool will be higher, resulting in increased axial force. As a consequence, axial force and torque are monitored at a tool rotation speed of 1,300 rpm and welding speed of 90 mm/min with plunge depth variation of 1.85–1.95 mm. It was found that all the welds are defect-free, and axial load and torque are almost constant as shown in Fig. 8. Similar observations are also seen with two other tool shoulder diameters (12 and 15 mm). Finally, the effect of shoulder diameter on axial force and toque is shown in Fig. 9. The effect of these three FSW tool shoulder (12, 15, and 18 mm) diameters is analyzed at a fixed tool rotation speed of 1,300 rpm, welding speed of 90 mm/min, and plunge depth of 1.9 mm. In this condition, defect-free welds are formed for all three shoulder diameters. The observation made is that, when tool shoulder diameter is increased, higher axial force and torque values are observed because of the higher reaction force given by the material to the tool and the higher friction existing at the interface.

Some of the results are consistent with results in literature. Ulysse [24] developed a model for the FSW process using three-dimensional visco-plastic modeling for butt joints made of aluminum plates and studied the effect of tool speed on temperature distribution and forces acting on the tool for various welding and rotational speeds. It was found that pin forces increase with increasing welding speeds, but the opposite effect was observed for increasing rotational speeds. Peel et al. [25] studied to produce good-quality welds for the friction stir welding of AA5083 to AA6082 at three different tool rotation speeds and welding speeds. They observed and compared the downward force; torque and power are at higher welding speed and lower rotational speed and vice versa. Cavaliere et al. [26] evaluated the welding speed effect on the mechanical and microstructural behavior of AA6082 welded plates with thickness of 4 mm. In addition, they also observed from the experimental results that force in Z-direction with increasing welding speeds (40 to 460 mm/min) at a fixed rotational speed of 1600 rpm is increasing. Cui et al. [27] studied on the FSW of aluminum alloy over a wide range of rotational speed and welding speed and measured the torque. It was found that an exponential decay model would be appropriate to describe the variation of torque with rotational speed and a linear fit for torque variation with respect to welding speed. A similar observation was seen in the present work also (see Figs. 5 and 6). But it was found from the present work that the torque variation with respect to welding speed is not purely linear. Upadhyay and Reynolds [28] studied the effects of thermal boundary conditions in friction stir-welded AA7050-T7 sheets and observed that the torque decreases with increasing tool rotation speed.

From the analysis, two different domains of FSW parameters are defined as shown in Fig. 10 for the formation of defective or defect-free welds. In order to have defect-free welds, welding should be performed at rotation speed of 1,300–1,500 rpm, welding speed of 80–120 mm/min, and plunge depth of 1.85–2 mm for the three different shoulder diameters (12, 15, and 18 mm).

From the results, the effect of plunge depth, shoulder diameter of tool, welding speed, and tool rotation speed plays a vital role to fabricate defect-free FSW joints. The function of the
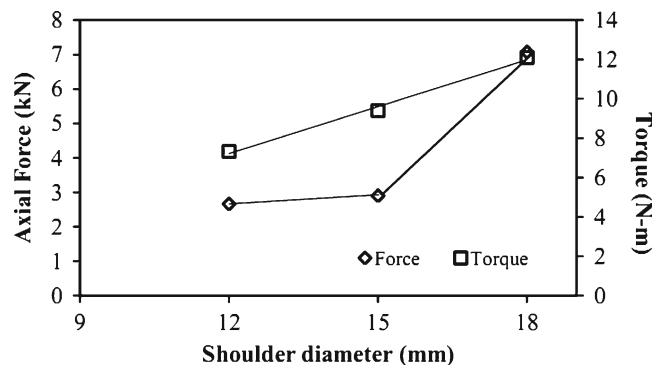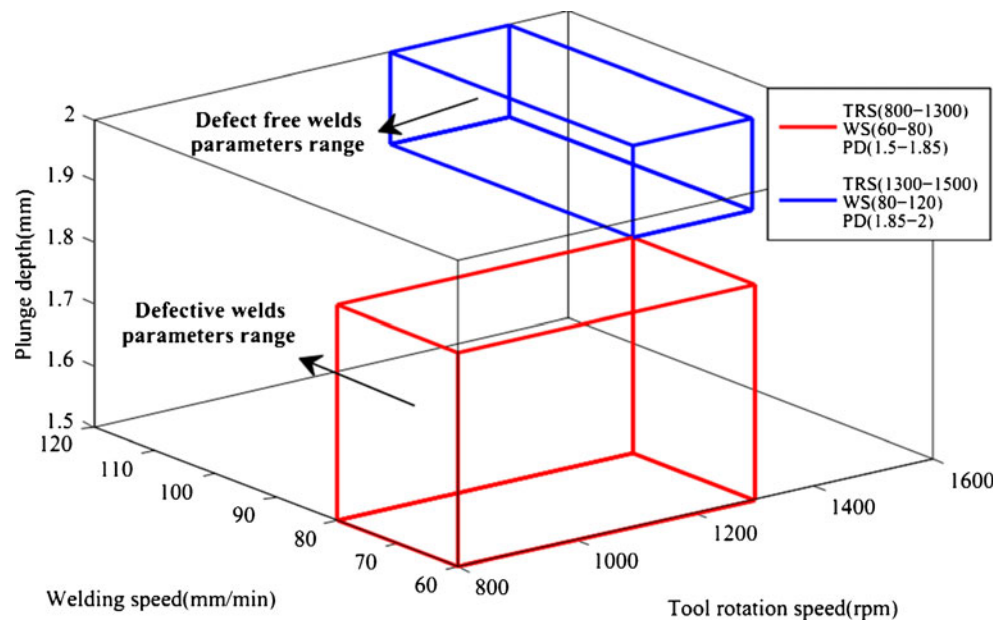

Fig. 9 Variations in force and torque of different FSW tool shoulder diameters (12, 15, and 18 mm) at 1,300 rpm tool rotation speed and 90 mm/min welding speed and 1.9 mm plunge depth. Error variation in force and torque is ±1 kN and ±1 Nm

Fig. 10 Domains of FSW parameters representing defective and defect-free weld parameters

non-consumable rotating tool pin is to stir the plasticized metal and move the same behind it. For this material, flow should be proper, which depends on the welding speed and tool rotation speed. They provide sufficient axial force, torque, and heat, resulting in defect-free welds. The tool shoulder diameter also affects the heat generated due to friction between the tool and sheet surface. The defects seen in FSW joints are due to lesser plunge depth, lesser shoulder contact area, slower welding speed, and low tool rotation speed. From the macrostructures, axial force, and torque analysis, the optimum range of welding parameters required for defect-free welds are obtained as shown in Table 7 for defect-free joints of AA 6061-T651 sheet material. It was also observed that the axial force and torque variation saturate after defect-free welds are formed as shown in Figs. 5, 6, 7, and 8. The axial force and torque saturate once tool rotation speed of 1,300 rpm, welding speed of 95 mm/min, and plunge depth of 1.85 mm are reached. Before this critical limit, a large variation in force and torque was witnessed. In fact, this is very clear from Fig. 8 where the axial force is almost a constant in the defect-free region with respect to plunge depth varying from 1.85 to 1.95 mm.

3.3 Condition for defect-free weld formation in FSW

In order to analyze the influence of rotational speed, welding speed, and plunge depth on the axial force and torque

Table 7 Selected optimum range of process parameters for FSW of AA 6061 sheets with thickness of 2.1 mm (defect-free weld formation range)

Shoulder diameter (mm)	Plunge depth (mm)	Rotation speed (rpm)	Welding speed (mm/min)
12, 15, 18	1.85–2.0	1,300–1,500	80–120

during the formation of defect-free welds, two trials have been carried out in the optimized range with 12 and 18 mm shoulder diameter tools by varying tool rotation speed within 1,300–1,800 rpm at 90 mm/min welding speed and 1.9 mm plunge depth, 80–150 mm/min welding speed at tool rotation speed of 1,300 rpm and 1.9 mm plunge depth, and plunge depth 1.85–2 mm at tool rotation speed of 1,300 rpm and 90 mm/min welding speed. At a different position of rotational speeds and welding speeds, axial force and torque are noted and plotted for both shoulder diameters
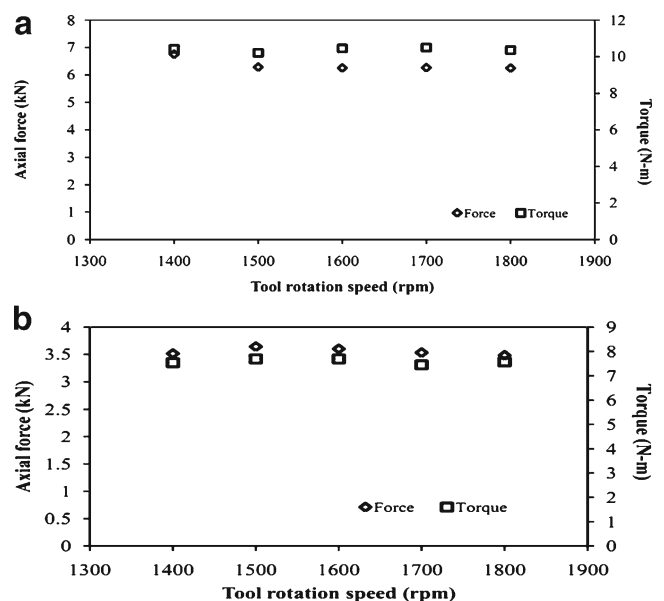

Fig. 11 Variations in force and torque generating defect-free welds at rotational speed of 1,400–1,800 rpm, welding speed 90 mm/min, and plunge depth of 1.9 mm. **a** 18 mm shoulder diameter. Error variation in force and torque is ±0.2 kN and ±0.2 Nm. **b** 12 mm shoulder diameter. Error variation in force and torque is ±1 kN and ±0.5 Nm
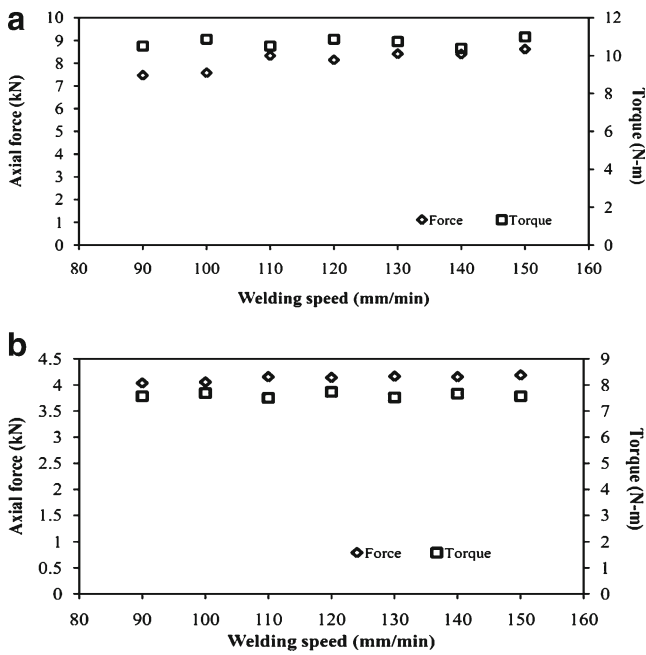
Fig. 14 Data obtained from machine for defective weld. Error variation in force and torque is ±1 kN and ±0.5 Nm

force and torque is relatively less and it is almost a constant. This is just opposite to the change in the axial force and torque presented in Fig. 5. Similar observations are seen with welding speed and plunge depth where defect-free welds are formed by comparing Fig. 6 with Fig. 12 and Fig. 7 with Fig. 13. Lesser variation in axial force and torque was observed in Figs. 12 and 13, while large variation was observed in the defective weld cases shown in Figs. 6 and 7.

From Figs. 5, 6, 7, and 8 and Figs. 11, 12, and 13, it was observed that the change in the axial force (∂F) and torque ($\partial \tau$) with respect to these three parameters (∂p) is high in defective FS welds and less in defect-free FS welds. Therefore, a simple criterion for identifying the defect-free weld region during FSW is given by:

$$\left(\frac{\partial \tau}{\partial p}\right)_{\text{defective}} > \left(\frac{\partial \tau}{\partial p}\right)_{\text{defect-free}}$$

and

$$\left(\frac{\partial F}{\partial p}\right)_{\text{defective}} > \left(\frac{\partial F}{\partial p}\right)_{\text{defect-free}} \tag{1}$$

where ∂p is change in welding speed or tool rotation speed or plunge depth.

Fig. 12 Variations in force and torque generating defect-free welds at a welding speed of 90–150 mm/min, tool rotation speed of 1,300 rpm, and plunge depth of 1.9 mm. **a** 18 mm shoulder diameter. Error variation in force and torque is ±1 kN and ±0.2 Nm. **b** 12 mm shoulder diameter. Error variation in force and torque is ±0.5 kN and ±0.5 Nm

as shown in Figs. 11 and 12. It is understood from Fig. 11 that, by increasing the tool rotation speed at constant welding speed and plunge depth, the change in axial
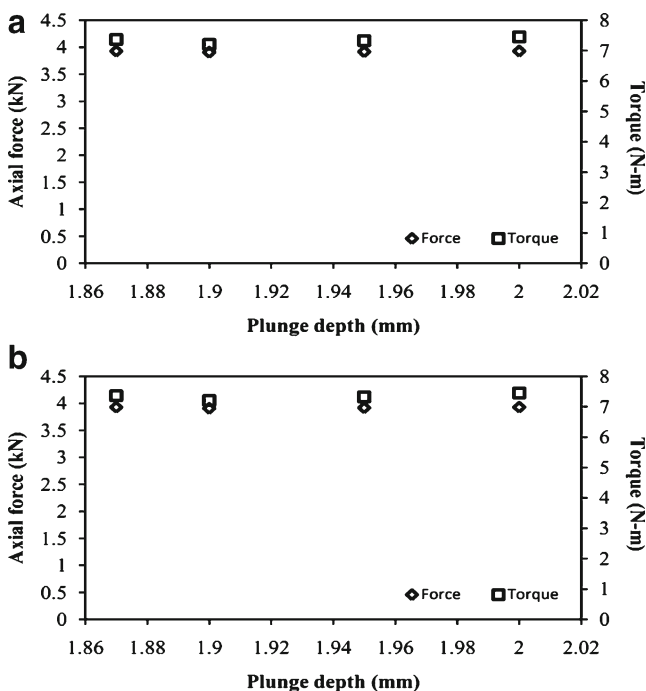

Fig. 13 Force and torque variations generating defect-free welds at a plunge depth of 1.85–2 mm, tool rotation speed of 1,300 rpm, and welding speed of 90 mm/min
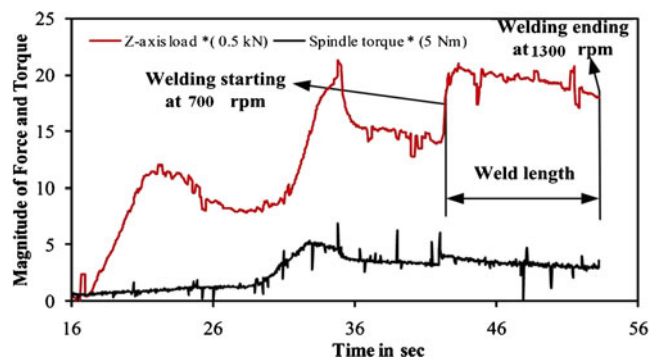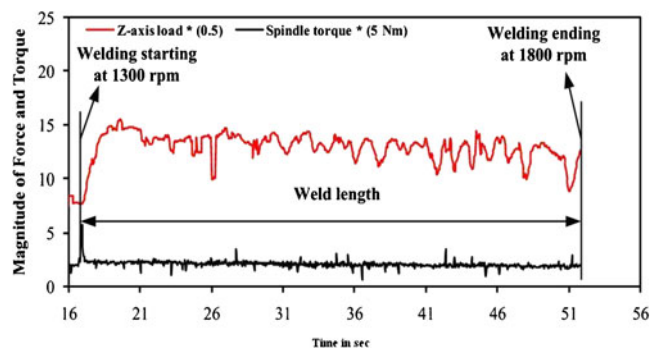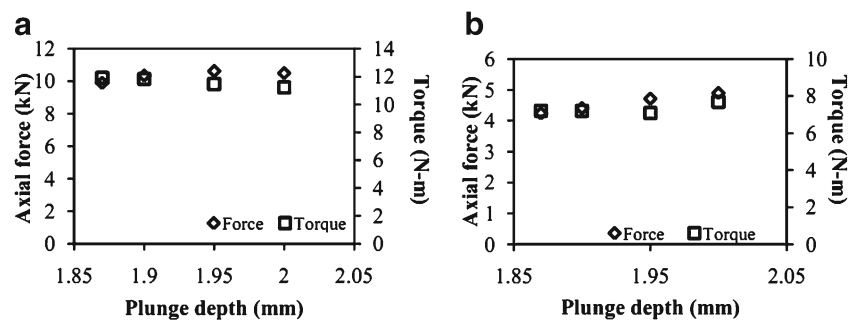

Fig. 15 Data obtained from machine for defective weld. Error variation in force and torque is ±1.5 kN and ±0.2 Nm

Fig. 16 Force and torque variations in the defect-free welds at a plunge depth of 1.85–2 mm, tool rotation speed of 1,300 rpm, and welding speed of 90 mm/min (for 5xxx base material)
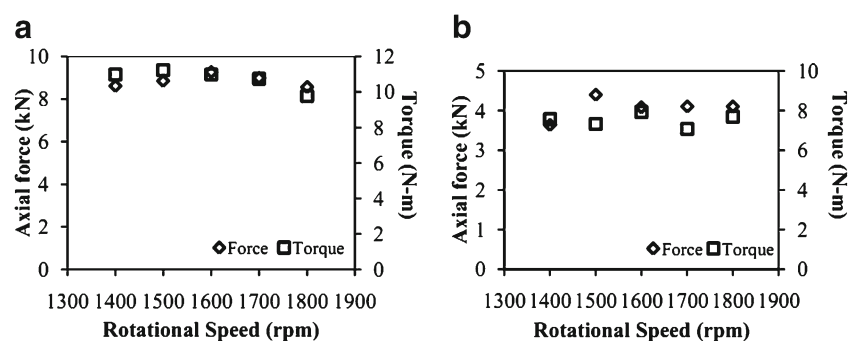

If the material volume available below the tool is less, which is the case in defective welds, the axial force, torque, will increase or decrease till it reaches an optimum parametric condition which gives a defect-free weld. Once a defect-free weld is attained, the material volume present below the tool will be a constant, and hence the axial force, torque values, will be maintained at a constant level relatively.

The criterion proposed should be independent of the materials that are fabricated by FSW process. This can be used as initial index to identify the onset of defect-free weld region. Later metallographic analysis can be performed within a small range of welding parameters as part of characterization. The axial force variation during actual welding trial is shown in Figs. 14 and 15, in which Fig. 14 is for defective weld with rotational speed starting at 700 rpm and ending at 1,300 rpm and Fig. 15 is for defect-free weld with rotational speed starting at 1,300 rpm and ending at 1,800 rpm. The data shown are directly obtained from the FSW machine. More variation in the force and torque is observed in the case of defective weld, whereas with rotational speed varying from 1,300 to 1,800 rpm, force and torque are relatively uniform, and in this range defect-free welds are formed.

A similar observation is also seen in the case of FSW blanks with AA 5xxx as base material. Figure 16 shows the variations of force and torque in the defect-free welds at plunge depth range of 1.85–2 mm, tool rotation speed of 1,300 rpm, and welding speed of 90 mm/min using two different shoulder diameters (12 and 18 mm). It was observed that variations in force and torque are almost constant. Figure 17 shows the variations of force and torque in the defect-free welds at rotational speed of 1,400–1,800 rpm, plunge depth of

1.9 mm, and welding speed of 90 mm/min using two different shoulder diameters (12 and 18 mm). Even in this case, force and torque are almost constant. From these observations, it is likely that the proposed criterion (Eq. 1) is independent of the material. In the defect-free range, axial force and torque remain constant, which can be considered as an initial index to identify the onset of a defect-free weld region. Figure 18a, b shows the macrostructures of FSW blanks made of Al 5xxx using 12 and 18 mm shoulder diameters at 1.95 plunge depth, indicating the absence of defects in the weld region. Similar results are seen in the case of Fig. 19a, b.

4 Conclusions

From the present work, the following important conclusions are made:

1. It was found from the analysis that, within the welding parameters range chosen, higher welding speed (80–120 mm/min), higher rotation speed (1,300–1,500 rpm), and higher plunge depth (1.85–2 mm) are preferred for producing a weld without internal defects. In the meantime, all the shoulder diameters (12, 15, and 18 mm) produced defect-free welds for AA6061-T6 sheet with 2.1 mm thickness used in the present work.
2. The axial force and torque are found to increase with an increase in welding speed and shoulder diameter. A decreasing trend is observed in axial force and torque while increasing the rotation speed. The axial force is found to increase with an increase in plunge depth, while there is no effect of plunge depth on the torque

Fig. 17 Variations in force and torque in defect-free welds at a rotational speed of 1,400–1,800 rpm, welding speed 90 mm/min, and plunge depth of 1.9 mm (for 5xxx base material). a Macrostructure at 12 mm shoulder diameter and 1.95 mm plunge depth. b Macrostructure at 18 mm shoulder diameter and 1.95 mm plunge depth

Fig. 18 Macrostructure of FSW blanks made of AA 5*xxx* using different shoulder diameters at constant plunge depth. **a** Macrostructure at 12 mm shoulder diameter and 1,600 rpm rotation speed. **b** Macrostructure at 18 mm shoulder speed and 1,600 rpm rotation speed

generated in FSW. These are the results observed during the formation of defective welds.

3. Once the optimized welding parameters are reached, there are no internal defects in the weld region. In this range of parameters, the axial force and torque are almost constant, indicating that they are insensitive to the change in welding parameters.

4. A simple criterion is proposed by observing the variation of axial force (F) and torque (τ) with respect to welding parameters (p) for identifying the onset of a defect-free weld region. The criterion is stated as:

$$\left(\frac{\partial \tau}{\partial p}\right)_{\text{defective}} > \left(\frac{\partial \tau}{\partial p}\right)_{\text{defect}-\text{free}}$$

and

$$\left(\frac{\partial F}{\partial p}\right)_{\text{defective}} > \left(\frac{\partial F}{\partial p}\right)_{\text{defect}-\text{free}}$$

5. The criterion is validated with welds made of a different base material (Al 5*xxx*) and the axial force and torque are found to remain constant while forming a defect-free weld region, indicating the validity of the criterion for another base material.
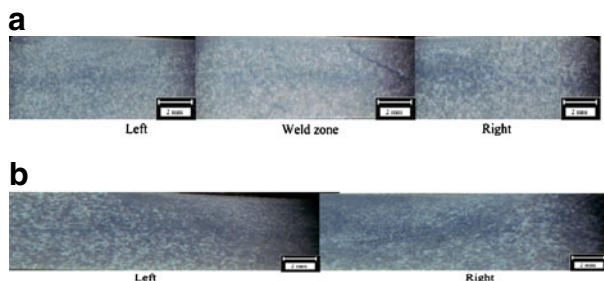

Fig. 19 Macrostructure of FSW blanks made of AA 5*xxx* using different shoulder diameters at constant tool rotation speed

References

1. Mathers G (2002) The welding of aluminium and its alloys. Woodhead, Cambridge
2. Zhi-hong F, Di-qiu H, Hong W (2004) Friction stir welding of aluminum alloys. J Wuhan Univ Technol, Mater Sci Ed 19:61–64
3. Mishra RS, Ma ZY (2005) Friction stir welding and processing. Mater Sci Eng R 50:1–78
4. Ma ZY (2008) Friction stir processing technology: a review. Metall and Mat Trans A 39A:642–658
5. Ghosh M, Kumar K, Kailas SV, Ray AK (2010) Optimization of friction stir welding parameters for dissimilar aluminum alloys. Mater Des 31:3033–3037
6. Scialpi A, De Filippis LAC, Cavaliere P (2007) Influence of shoulder geometry on microstructure and mechanical properties of friction stir welded 6082 aluminium alloy. Mater Des 28:1124–1129
7. Elangovan K, Balasubramanian V (2008) Influences of tool pin profile and tool shoulder diameter on the formation of friction stir processing zone in AA6061 aluminium alloy. Mater Des 29:362–373
8. Kumar K, Kailas SV (2008) The role of friction stir welding tool on material flow and weld formation. Mater Sci Eng, A 485:367–374
9. Fujii H, Cui L, Maeda M, Nogi K (2006) Effect of tool shape on mechanical properties and microstructure of friction stir welded aluminum alloys. Mater Sci Eng, A 419:25–31
10. Elangovan K, Balasubramanian V, Valliappan M (2008) Influences of tool pin profile and axial force on the formation of friction stir processing zone in AA6061 aluminium alloy. Int J Adv Manuf Technol 38:285–295
11. Zhang Z, Liu YL, Chen JT (2009) Effect of shoulder size on the temperature rise and the material deformation in friction stir welding. Int J Adv Manuf Technol 45:889–895
12. De Giorgi M, Scialpi A, Panella FW, De Filippis LAC (2009) Effect of shoulder geometry on residual stress and fatigue properties of AA6082 friction stir welded joints. J Mech Sci Technol 23:26–35
13. D'Urso G, Giardini C (2010) The influence of process parameters and tool geometry on mechanical properties of friction stir welded aluminum lap joints. Int J Mater Form 3(1):1011–1014
14. Arora A, De A, DebRoy T (2011) Toward optimum friction stir welding tool shoulder diameter. Scr Mater 64:9–12
15. Ren SR, Ma ZY, Chen LQ (2007) Effect of welding parameters on tensile properties and fracture behavior of friction stir welded Al–Mg–Si alloy. Scr Mater 56:69–72
16. Rodrigues DM, Loureiro A, Leitao C, Leal RM, Chaparro BM, Vilaça P (2009) Influence of friction stir welding parameters on the microstructural and mechanical properties of AA 6016-T4 thin welds. Mater Des 30:1913–1921
17. Cavaliere P, Campanile G, Panella F, Squillace A (2006) Effect of welding parameters on mechanical and microstructural properties of AA6056 joints produced by friction stir welding. J Mater Process Technol 180:263–270
18. Liu FC, Ma ZY (2008) Influence of tool dimension and welding parameters on microstructure and mechanical properties of friction-stir-welded 6061-T651 aluminum alloy. Metall Mater Trans A 39A:2378–2388
19. D'Urso G, Ceretti E, Giardini C, Maccarini G (2009) The effect of process parameters and tool geometry on mechanical properties of

friction stir welded aluminum butt joints. Int J Mater Form 2 (1):303–306

20. Zimmer S, Langlois L, Laye J, Goussain JC, Martin P, Bigot R (2009) Influence of processing parameters on the tool and work-piece mechanical interaction during friction stir welding. Int J Mater Form 2(1):299–302

21. Sakthivel T, Sengar GS, Mukhopadhyay J (2009) Effect of welding speed on microstructure and mechanical properties of friction-stir-welded aluminum. Int J Adv Manuf Technol 43: 468–473

22. Rajamanickam N, Balusamy V, Madhusudhanna Reddy G, Natarajan K (2009) Effect of process parameters on thermal history and mechanical properties of friction stir welds. Mater Des 30:2726–2731

23. Rhodes CG, Mahoney MW, Bingel WH, Spurling RA, Bampton CC (1997) Effects of friction stir welding on microstructure of 7075 aluminum. Scr Mater 36:69–75

24. Ulysse P (2002) Three-dimensional modeling of the friction stir-welding process. Int J Mach Tool Manuf 42:1549–1557

25. Peel MJ, Steuwer A, Withers PJ, Dicker Son T, Shi Q, Sher Cliff H (2006) Dissimilar friction stir welds in AA5083-AA6082. Part I: process parameter effects on thermal history and weld properties. Metall and Mat Trans A 37A:2183–2193

26. Cavaliere P, Squillace A, Panella F (2008) Effect of welding parameters on mechanical and microstructural properties of AA6082 joints produced by friction stir welding. J Mater Process Technol 200:364–372

27. Cui S, Chen ZW, Robson JD (2010) A model relating tool torque and its associated power and specific energy to rotation and for-ward speeds during friction stir welding/processing. Int J Mach Tool Manuf 50:1023–1030

28. Upadhyay P, Reynolds AP (2010) Effects of thermal boundary conditions in friction stir welded AA7050-T7 sheets. Mater Sci Eng, A 527:1537–1543